All-solid-state silver batteries assembled by Spark Plasma Sintering

G. Delaizir [1], N. Manafi, G. Jouan, P. Rozier, M. Dollé *

Centre d'Elaboration de Matériaux et d'Etudes Structurales (CEMES-CNRS), UPR CNRS 8011, Université de Toulouse, Toulouse, 31055 Cedex 4, France

ARTICLE INFO

Keywords:
Solid state battery
Spark plasma sintering
Interface
Structural characterization

ABSTRACT

Bulk type $Ag_{0.7}V_2O_5//Ag_6I_4WO_4//Ag_{0.7}V_2O_5$ all solid state batteries have been assembled in one step by Spark Plasma Sintering (SPS). Their electrochemical performances were compared to the ones of similar solid state cells assembled by cold pressing, as reported in the 90s. The cold pressed all solid state batteries with thick composite electrodes (above 400 μm) display poor electrochemical properties explained by an important cell polarization associated to poorly defined electrode/electrolyte interfaces. In contrary, the thick batteries obtained by SPS exhibit excellent reversibility without any need of pressure load during cycling. The behavior lies on the well defined interfaces and a good mechanical aspect, which are kept upon cycling. During the charge/discharge cycles, the electrochemical formation of $Ag_xV_2O_5$ does not display a drastic volume change, preserving the electrode/electrolyte interfaces. The structural evolution of $Ag_xV_2O_5$ upon cycling is discussed in comparison to the known phases synthesized by solid state reactions. The obtained results on silver batte ries allow a general reflection on the development of all solid state Li ion technology by SPS.

1. Introduction

Recent observations confirm that the world's oil and natural gas supplies are running out too fast and, soon they will fall below the level required to meet international demands. It appears critical to consider ecological electricity generation systems (photovoltaic, windmill, geothermic energy…) and to associate them with energy storage systems. Rechargeable batteries or accumulators are the old est form of electricity storage and the most widely used. Despite im portant progresses over the last twenty years, the improvements of conventional liquid/gel based Li ion batteries are slowing down and breakthroughs are needed. In regards to tomorrow's energy needs, it is necessary to develop energy storage systems with high energy densities, long life, low cost, little or no maintenance and a high de gree of safety. All solid state batteries may meet these requirements because of their low loss of capacity as a function of time [1], their thermal stability, their absence of leakage and pollution (solvent free). However, the energy densities of such technology remain restricted, mainly due to limitations in their development. Since 1982, all solid state thin film batteries have always been under sig nificant improvements but their energy densities are still too low for large applications. Over the last fifty years, various solid electro lyte cells based either on Ag^+, Cu^+ or Li^+ ions were reported [2 4] with, however, independently of the ion, limited energy densities. These limitations were due to the necessity to use thin electrodes needed to minimize the polarization due to the resistive electrode/ electrolyte interfaces of the cells assembled by cold compaction. Recently, we reported a new approach to develop bulk type all solid state Li ion batteries using the Spark Plasma Sintering (SPS) technique [5]. The SPS allows achieving cells with 100 to 800 μm thick composite electrodes with a compactness ranging from 75 to 90%. It was shown that these batteries offer interesting electrochem ical behavior at temperatures above 80 °C, which was necessary to reach an ionic conductivity above 10^{-3} S.cm^{-1} with our crystalline Nasicon type solid electrolyte. Amongst the known solid electrolytes, silver and copper ion conductors exhibit very high ionic conductivity at room temperature, about 0.05 S.cm^{-1} for the glassy $Ag_6I_4WO_4$ [6] and 0.34 S.cm^{-1} for the crystalline $Rb_4Cu_{16}I_7Cu_{13}$ [7]. In comparison, glass ceramics Li_2S P_2S_5 present conductivity of about 10^{-4} S.cm^{-1} at 25 °C, while being difficult to obtain and moisture sensitive. While waiting for the finding of optimized Li ion conductor, our inter est was to investigate electrochemical systems operating at room temperature and to compare identical thick cells assembled either by cold compaction or by SPS.

Given that the assembly by SPS implies to work in a conducting die, the all solid state cells have to be prepared in the discharged state. Symmetric cells using the same active material for the positive and the negative electrode are then perfectly adapted. In regards to previous reported investigations by cold compaction, symmetric sil ver cells $Ag_{0.7}V_2O_5//Ag_6I_4WO_4//Ag_{0.7}V_2O_5$ [8,9] present the advantage to be stable in open air. Despite its poor interest in regards to applica tions, such system is ideal for the fundamental study of all solid state technology as it considers the use of a glass ceramic electrolyte in comparison to our previous work on crystalline solid electrolyte. This electrolyte presents a low melting temperature leading to self

* Corresponding author. Tel.: +33 5 62 25 78 11; fax: +33 5 62 25 79 99.
E-mail address: mickael.dolle@cemes.fr (M. Dollé).

[1] Permanent address: Groupe d'Étude des Matériaux Hétérogènes (GEMH), ENSCI, Centre Européen de la Céramique, 87068 Limoges Cedex, France.

doi:10.1016/j.ssi.2011.11.012

supported cells sintered at temperature low enough to prevent sec ondary reactions such as reduction by the graphite die and enables the use of a wider range of active materials. The selected silver cell is also interesting regarding the possible mechanical stress, which can be generated at the electrode/electrolyte interface upon cycling with the electrode material "breathing". Takada et al. [8,9] reported a phase transition upon cycling, which is expected for $Ag_xV_2O_5$ at $x = 0.66$ [10] in compounds made by solid state chemistry. Therefore, despite an important volume change occurring inside the composite electrodes upon cycling, it did not affect the cyclability of their all solid state batteries assembled by cold compaction. The impact of such volume change on all solid state batteries assembled by SPS is then considered and discussed in this paper. In order to estimate the cell volume of the different compounds, $Ag_xV_2O_5$ ($x \leq 0.7$) were characterized after preparation by chemical extraction from $Ag_{0.7}V_2O_5$ to mimic the electrochemical oxidation. In regards to the obtained results, a general reflection on the development of all solid state batteries by SPS is then proposed.

2. Experimental procedure

2.1. Synthesis of electrode and electrolyte materials

The electro active material, $Ag_{0.7}V_2O_5$ is obtained by mixing silver metal powder (Alfa Aesar, 99.9%) and vanadium pentoxide, V_2O_5 (Al drich, 99.6%) in stoichiometric amount. The mixture is introduced in a silica tube and placed under primary vacuum. The silica tube is then sealed and heated at 600 °C overnight.

The electrolyte, $Ag_6I_4WO_4$ is synthesized from the precursors $AgNO_3$ (Strem Chemicals, 99.9%), $Na_2WO_4{,}2H_2O$ (Sigma Aldrich, 99%) and KI (Sigma Aldrich, 99%) in stirred distilled water. The yel low mixture is then washed several times with distilled water, dried and introduced in a silica tube. The tube is sealed under vacuum and heated at 400 °C for 18 h. The melt is quenched by dropping the tube into cold water to obtain the glass.

The composite electrodes (positive and negative) are obtained by mixing $Ag_{0.7}V_2O_5$ and $Ag_6I_4WO_4$ (1:1 ratio in wt.%) in a planetary ball milling apparatus using agate mortars for 2 h. The weight ratio for positive and negative electrode is 1:2. Typically, the weights used for batteries assembled in Ø8mm diameter die by SPS were 0.15 g for positive electrode, 0.30 g for negative electrode and 0.2 g for the electrolyte.

2.2. Chemical extraction

Chemical extraction of $Ag_{0.7}V_2O_5$ was performed to mimic the electrochemical oxidation. $Ag_{0.5}V_2O_5$, $Ag_{0.4}V_2O_5$, $Ag_{0.3}V_2O_5$ and V_2O_5 were synthesized by using 1 M NO_2BF_4 acetonitrile solutions as the oxidizing agent; the NO_2^+/NO_2 couple was the active redox couple, while the BF_4^- ions solely act as spectators.

$$Ag_{0.7}V_2O_5 \rightarrow Ag_{0.7-x}V_2O_5 + xAg^+ + xBF_4^- + xNO_2\uparrow$$

The experiment was conducted at 80 °C for 48 h in an argon dry box by stirring in a glass vessel 0.5 g of $Ag_{0.7}V_2O_5$ and 30 mL acetoni trile solution containing the right amount of oxidizing agent accord ing to the above reaction.

2.3. Spark Plasma Sintering

Silver solid state batteries were assembled using Spark Plasma Sintering equipment (Dr. Sinter 2080 Syntex machine) of the "Plate forme Nationale de Frittage Flash CNRS". The experiments were conducted using graphite die with 8 mm inner diameter closed by graphite punches at both sides and placed in a vacuum chamber. While a uniaxial pressure is applied following a program described in the discussion part, the heating is generated by sequences of DC pulses with adapted intensity to respect the expected temperature evolution. A configuration of 12 pulses (each of 3.3 ms) followed by two periods (6.6 ms) of zero current was used. The effective sample temperatures are estimated roughly equal to the one measured at the surface of the die. Though a gradient is possible previous experi ments show that in the investigated range of temperature it can be considered as negligible [11]. The evolution of the sample is followed by measuring the displacement as a function of time and then as a function of temperature and pressure.

2.4. Characterizations

XRD patterns were recorded at room temperature in the 2θ range 10 50° using a SEIFERT XRD 3000 diffractometer with a graphite monochromatized Cu Kα radiation.

DSC measurements were performed on the electrolyte using a TA Instrument Q1000 equipment with the heating rate of 10 °C/min.

Interfaces of both batteries (made by SPS and cold pressing) were analyzed by Scanning Electron Microscopy (JEOL JSM 6490).

Electrochemical measurements were carried out in galvanostatic mode using a Biologic VSP potentiostat. Prior to the cycling, a layer of platinum was deposited on both sides of the batteries to act as cur rent collectors. Potential/composition curves were registered be tween 100 mV and 500 mV at 20 °C in air.

3. Results and discussion

3.1. Battery assembly

SPS process implies sample's heating by current pulses, which go through a conducting die and the sample itself if it is electronic con ductor. Thus prior to any assembling of full cell, the behavior of each material (active material and electrolyte) is investigated alone and included in mixtures corresponding to the composite electrode materials. Experiments show that in agreement with their respective melting temperature evolution, the electrolyte $Ag_6I_4WO_4$ presents the lowest sintering temperature (210 °C), which occurs via a viscous flow mechanism. The electrolyte being included in the different com ponents (composite electrode), it is expected to act as a binder insur ing the cohesiveness of the full cell. To minimize possible parasitic reaction, the maximal temperature is then settle to 210 °C while a constant load of 75 MPa is applied for all the experiments. The behav ior of the composite electrode (active material and electrolyte) is in vestigated following the optimized process. XRD patterns of the obtained samples before and after the SPS experiments are reported in Fig. 1. While being mainly glassy, as confirmed by our DSC

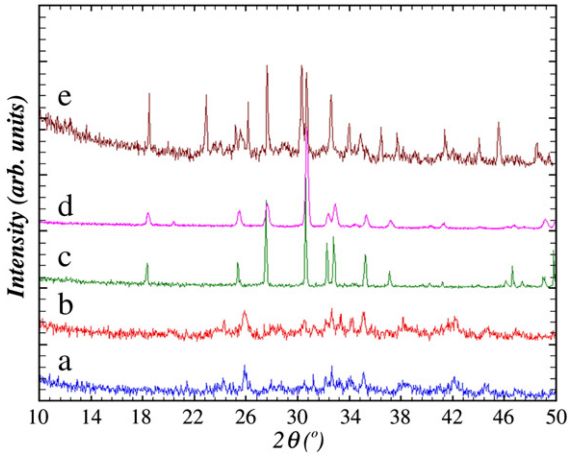

Fig. 1. SPS matrix set-up to assemble silver solid state batteries.

measurements ($T_g = 120$ °C, $T_c = 140$ °C), the as prepared electrolyte presents a XRD pattern with small diffraction peaks (Fig. 1a), also observed in the sample prepared by Takada et al. [8,9]. These peaks are associated to $Ag_{26}I_{18}W_4O_{16}$ (ICDD PDF 01 073 8501) in agreement with the work of Chan et al. [12]. After the SPS experiment at 210 °C, the XRD pattern obtained on a $Ag_6I_4WO_4$ pellet looks similar to the powder and it indicates no important modification occurs in the SPS (Fig. 1b). The same check on $Ag_{0.7}V_2O_5$ was carried out (Fig. 1c and d) and it confirms the silver vanadium bronze does not evolve upon the SPS experiment. However, it is important to note the preferred orientation observed on the $Ag_{0.7}V_2O_5$ pellet, which is especially visible by the intensity change of the (003) peak at 30.7°(2θ) in comparison to the other diffraction peaks. This result is explained by the lamellar structure of $Ag_{0.7}V_2O_5$ along the c axis, which forms platelets tending to align perpendicularly to the applied pressure. The XRD pattern of the ground composite electrode after SPS (Fig. 1e) is characteristic of a pellet containing the silver vanadium bronze $Ag_{0.7}V_2O_5$ and $Ag_{26}I_{18}W_4O_{16}$, both in a glassy matrix. This result confirms no chemical reaction occurs upon the SPS sintering despite a higher crystallization of $Ag_{26}I_{18}W_4O_{16}$. This fast crystallization in the SPS was already observed on other amorphous materials as we report such crystallization on infrared glass ceramics [14]. This presence of more $Ag_{26}I_{18}W_4O_{16}$ crystals in the composite electrode is not harmful to the cells performance, as this phase is the conducting phase in the $Ag_6I_4WO_4$ composition [13].

As a final step, full cells are assembled using the optimized parameters. The stacking of composite electrode and electrolyte prepared as described in Section 2.1 are successively introduced in the graphite die and placed in the SPS chamber. The pressure is applied during the first stage of the heating process (Fig. 2), reaches the maximal 75 MPa value when the temperature is 100 °C and is then kept constant. The temperature is increased up to 210 °C in 7 min maintain constant for 2 min before cooling following the inertia. The evolution of the sample displacement is reported in Fig. 3. It indicates that even though as expected a compaction of the sample is observed during the application of the pressure, the displacement increases while the pressure is kept constant. This indicates the existence of a sintering process confirmed by the mechanical behavior of the obtained pellet as well as its thickness 2.0 mm.

To compare batteries performances made by SPS to the one described in the literature [8,9], solid state batteries are assembled using cold pressing (Ø13 mm). The powdered samples (electrolyte and composite electrode) and the 1:2 positive:negative electrode ratio are kept identical while the weight of each component is

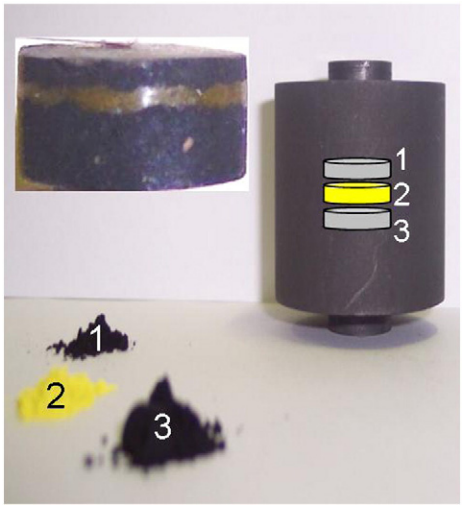

Fig. 2. XRD patterns of the electrolyte $Ag_6I_4WO_4$ alone before (a) and after SPS (b), $Ag_{0.7}V_2O_5$ alone before (c) and after SPS (d) and the composite electrode after SPS (e).

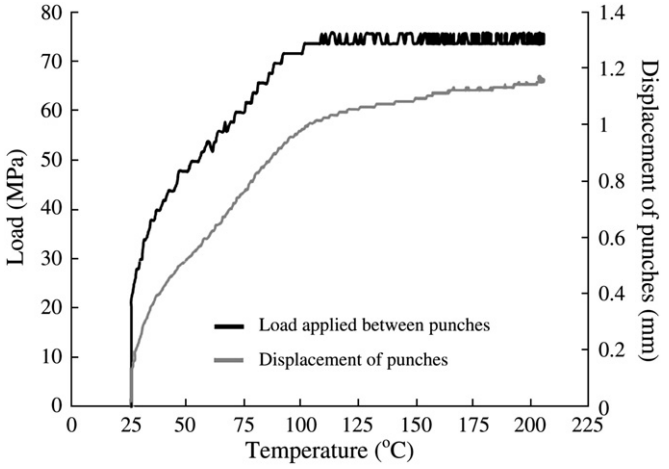

Fig. 3. SPS parameters during assembling of the battery.

calculated to take into account the increase of the die diameter and make comparable the thickness of obtained pellets. While the pressure is four times higher than the one applied during SPS experiment and despite a relatively good mechanical aspect the thickness of the obtained pellets is 2.7 mm indicating compactness 35% lower than using SPS experiment. This large decrease is of course related to the absence of sintering ("cold" treatment) and confirms the benefit of short time heat treatment.

3.2. Characterization of interfaces

Interfaces between composite electrodes and the electrolyte (cross section) for both batteries (made by SPS and cold pressing) observed using SEM techniques (Fig. 4). SEM pictures confirm that despite really short the SPS heat treatment induces a great evolution of interfaces. The numerous cracks observed in the composites electrodes after cold pressing have disappeared in the SPS sample showing cleaner and better defined interfaces. As the cracks induce kinetic limitations and then important cell polarization, one can expect that the use of SPS will drastically improve the electrochemical performances of silver solid state batteries.

3.3. Electrochemical tests

As deduced from previous investigations the solid state batteries assembled by cold pressing present high polarization, the electrochemical investigations were carried out with a maximal current density of 38 $\mu A.cm^{-2}$ and with the use of a constant load applied on the cells to ensure better interfacial contacts. Despite these testing conditions, a poor capacity was delivered by cold compacted cells (Fig. 5). In contrary, the batteries made by SPS were tested without any load and at higher current densities (100 and 300 $\mu A.cm^{-2}$) confirming the benefit of the short SPS heat treatment. The batteries were then tested in the potential range 100 500 mV after a partial charge at 50 $\mu A.cm^{-2}$, which lead the batteries to the composition $Ag_{0.55}V_2O_5$ (+)/$Ag_{0.775}V_2O_5$ (−). Fig. 6 show potential composition curves of batteries made by Spark Plasma Sintering under two different current densities. The positive electrode of batteries assembled by SPS exchange 0.12 electron under 100 $\mu A.cm^{-2}$ and 0.08 electron under 300 $\mu A.cm^{-2}$, which correspond to batteries with a respective composition after charge of $Ag_{0.43}V_2O_5$ (+)/$Ag_{0.835}V_2O_5$ (−) under 100 $\mu A.cm^{-2}$ and of $Ag_{0.47}V_2O_5$ (+)/$Ag_{0.815}V_2O_5$ (−) under 300 $\mu A.cm^{-2}$. The electrochemical curve under 100 $\mu A.cm^{-2}$ displays a change in the slope at the composition close to $Ag_{0.5}V_2O_5$, in good agreement with previous published results [8,9].

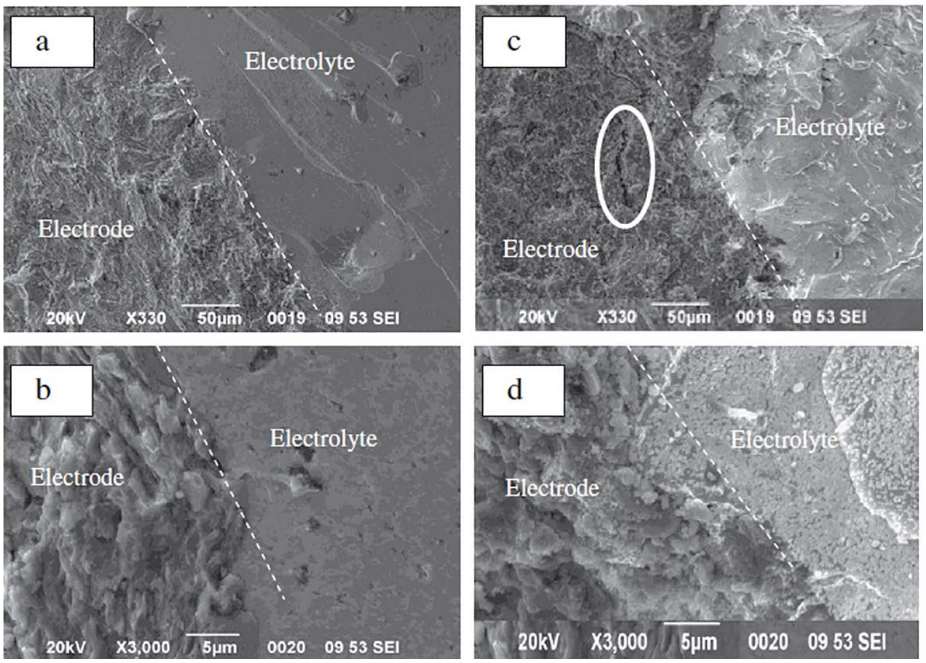

Fig. 4. Interfaces between electrode and electrolyte in batteries made by SPS (a) and (b) and cold pressing (c) and (d).

It is always difficult to compare electrochemical solid state devices as such technology requires a large grain boundaries density between electrode and electrolyte, which will depend on the powders size distribution and the way to mix materials together to ensure the electronic and ionic percolation through the composite electrode volume. Thus, the optimized electrode formulation of 50/50 (wt.%) used by Takada et al. [8,9] is certainly not the optimized one for thick composite electrodes, which may explain why our SPS prototypes exchange less Ag ions than thin cold compacted cells when charge to 0.5 V.

Despite the use of non optimized composite electrodes, the different behavior observed between cold compacted cells (Fig. 5) and cells obtained by SPS (Fig. 6) clearly demonstrates that the cold compaction method cannot be efficiently used for thick batteries despite its use remains interesting for thin all solid state batteries. The main explanation for such difference lies on the electrode/electrolyte interface quality after the assembly by SPS, which allows minimizing the internal resistance of the composite electrodes. Then to answer the need for higher energy densities, id est thicker electrode, the use of SPS appears promising in association to the research of an optimized formulation for the composite electrodes.

Surprisingly, the electrochemical curves observed in the case of batteries made by SPS show good reversibility despite the expected volume change of the positive electrode upon charge. This volume change, expected at $x = 0.66$ on materials prepared by solid state reaction [9], should lead to contact loss between the electrode material and the electrolyte, which would drive to significant capacity loss even after 10 cycles due to cracks formation in the composite electrodes. As no evidence for such phenomena is observed, the structural evolution of $Ag_{0.7}V_2O_5$ upon charge is investigated.

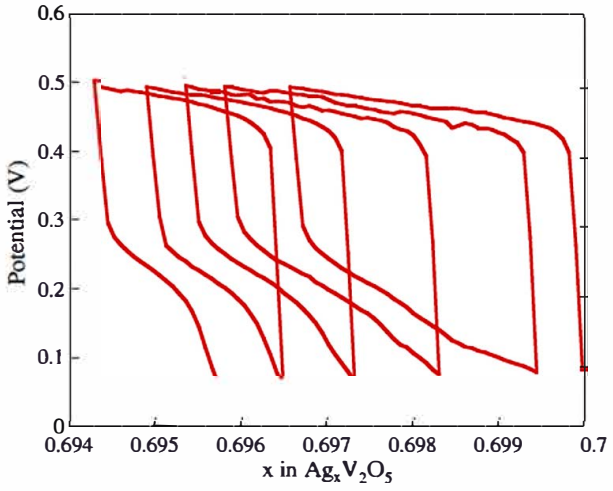

Fig. 5. Charge–discharge cycles of the batteries assembled by cold pressing at 20 °C in open air at constant current (50 µA) 2.5 mm thick battery.

3.4. Structural evolution investigation

The volume change reported in the literature [8] has been related to the existence, during electrochemical process, of the phase transition δ $Ag_xV_2O_5$ to β $Ag_xV_2O_5$. These phases have been evidenced by Galy et al. [10] during the investigation using high temperature solid state routes of the Ag_2O V_2O_5 V_2O_4 system. The β $Ag_xV_2O_5$ presents a homogeneity domain limited at $x = 0.66$ for the upper value. This limit corresponds to the full occupancy of the tunnels running along the [010] direction defined by the VO tridimensional host network (Fig. 7a). The δ $Ag_xV_2O_5$ phase is built up with layered V_4O_{10} host network (Fig. 7b). The silver cations lying in the interlayer space insure the cohesion of the structure. The full occupancy of Ag^+ site leads to the $x = 1$ upper limit of this phase. Takada et al. [8,9] reported that electrochemical extraction of silver from this latter phase drives to structural change that they interpreted as related to the existence even at low temperature of the δ to β transition.

In our case, despite a slight change in the electrochemical curves located close to 0.66, the absence of capacity loss indicates that this change does not induce physical destruction of the electrode/electrolyte interfaces. To get a better understanding of the structural effect of silver extraction, $Ag_xV_2O_5$ ($x<0.7$) compounds were prepared by

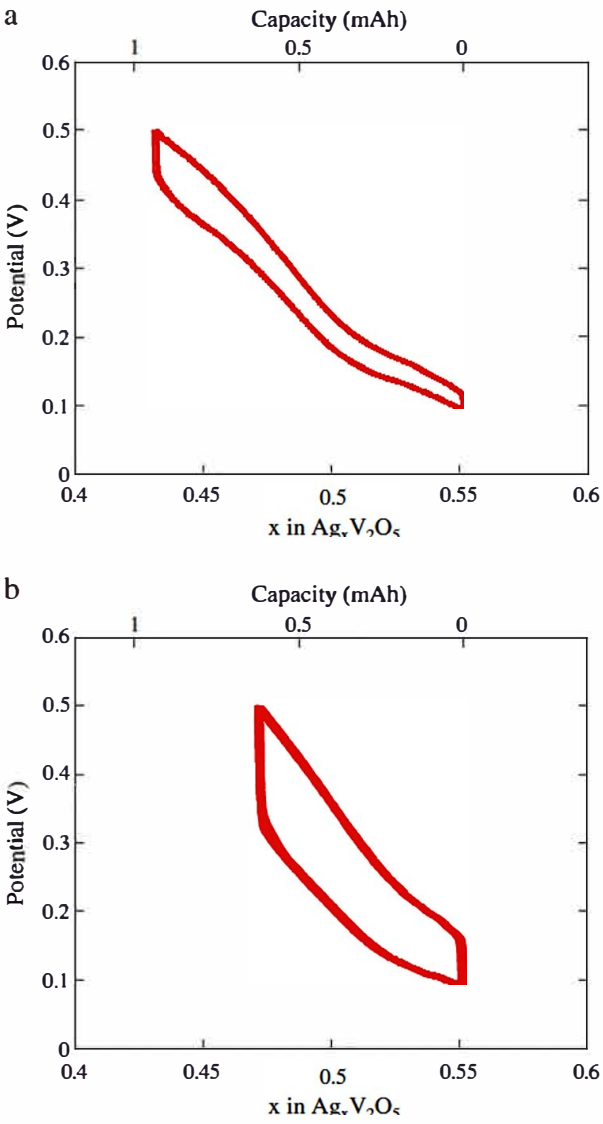

Fig. 6. Charge–discharge cycles of the batteries assembled by Spark Plasma Sintering at 20 °C (a) at constant current of 50 μA (c) at constant current of 150 μA.

chemical extraction to mimic the low temperature electrochemical process. The XRD patterns of samples corresponding to different steps in the chemical extraction are represented in Fig. 8. Obviously some changes occur especially at about the $x = 0.4$ composition. However careful examination of patterns obtained for silver content below this limit can be interpreted without drastic structural

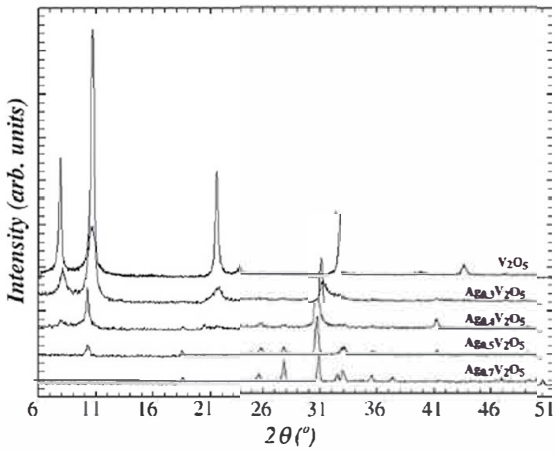

Fig. 8. X-ray diffraction pattern of chemical extracted phase from δ $Ag_{0.7}V_2O_5$.

transition. The low quality of XRD patterns related to the low temperature process prevent for full structural refinement but these XRD patterns are enough to interpret in a reliable way the structural evolution. In a first stage, starting with δ $Ag_{0.7}V_2O_5$ compound, the chemical extraction operates in a solid solution mode with a smooth evolution of the cell parameters, which are reported for some compositions in Table 1. Then, for lower silver content extra peaks are observed. To interpret this new pattern, we first check the possibility to fit it using the calculated pattern of the β $Ag_xV_2O_5$ phase. In that case, despite some agreement between calculated and experimental Bragg peaks, a full agreement is not obtained. Moreover the cell parameters refined to take into account the Bragg peaks position lead to cell volume and inter atomic distances far from realistic ones. The second hypothesis was then to consider a monotonous silver extraction process associated to the loss of C centering. This loss induces non equivalence of structural factors responsible for the suppression of systematic absences explaining the growing of new Bragg peaks (Fig. 9). Taking into account cell parameters evolution as well as symmetry loss and preferential orientation allow obtaining a good agreement between calculated and experimental XRD pattern (Fig. 9c). The low temperature extraction of silver from δ $Ag_xV_2O_5$ proceed through a monotonous mechanism involving smooth gliding of the V_4O_{10} layers that can be associated to ordering of the remaining silver cations. These successive ordering and their consequences on the observed crystallographic symmetries can account for the existence of pseudo biphasic domains as observed on the electrochemical curve. However, during the whole extraction insertion (charge discharge) process of a full cell, the formation of $Ag_xV_2O_5$ ($0.43 < x < 0.55$) at the positive electrode induces a progressive slight volume change, which does not degrade the electrode/electrolyte interfaces.

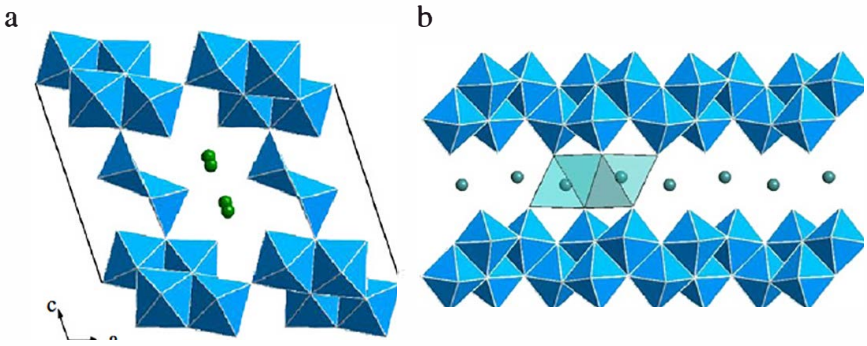

Fig. 7. Structure projection onto the (010) plane of β-$Ag_xV_2O_5$ (a) and δ-$Ag_xV_2O_5$ (b).

Table 1
Calculated lattice parameters for the initial δ-$Ag_{0.7}V_2O_5$ and the extracted phase $Ag_{0.5}V_2O_5$ and $Ag_{0.4}V_2O_5$.

Phase	Lattice			
	a (Å)	b (Å)	c (Å)	β (°)
$Ag_{0.7}V_2O_5$ C2/m δ phase	11.69	3.67	8.77	90.51
$Ag_{0.5}V_2O_5$ C2/m δ phase	11.59	3.65	8.71	90.54
$Ag_{0.4}V_2O_5$ P2/m δ phase	11.60	3.66	8.71	90.56
$Ag_{0.4}V_2O_5$ P2/m β phase	12.00	3.60	9.00	109.00

Standard deviation over estimated to ±10 $^{-2}$.

4. Conclusion

As recently demonstrated, the Spark Plasma Sintering (SPS) technique allows developing bulk type all solid state batteries in short times (few minutes). Silver all solid state batteries can be assembled in one step SPS when appropriate electrode and electrolyte materials are chosen. The comparison with cells obtained by cold pressing indicates that the short time heat treatment characteristic of SPS process allows the development of thick batteries with good electrochemical properties, in contrary to the cold compaction approach that is restricted to thinner systems to limit the kinetic limitations. The present study also points out that the development of thick all solid state batteries implies to consider cautiously the electrode composite formulation, as an optimized formulation for thin all solid state batteries may not be optimized for thick systems, which require a complete investigation of ionic and electronic paths through the electrode composite volume. Thick batteries performances are explained by the high quality of the electrode/electrolyte interfaces generated by SPS that can be kept upon cycling even in case of small volume change during electrochemical process. More important, in the present paper, we show the use of a glass ceramic electrolyte with a low melting temperature leads to self supported cells at relatively low temperature (210 °C). This temperature is low enough to prevent possible reaction between active material, especially oxides, and graphite (die) heated in reducing atmosphere.

These results, obtained using a model system, can then be used to define requirements to the improvement of more interesting systems such as Li based ones. The search for a Li based solid electrolyte (with ionic conductivity $>10^{-3}$ S.cm^{-1} at room temperature), which could be sintered at a temperature below the known reacting temperature of oxide with carbon would be of first interest. Regarding the known electrolytes, few of them may suit these requirements among them the promising Li_2S P_2S_5 glass ceramics. Despite, a complex preparation under inert atmosphere and a possible crystallization of non conductive phases [15], recent results confirmed "all solid state" Li ion batteries may be assembled by hot press technique at low temperature (210 °C) using such glass ceramics [15]. These results support our SPS approach and the need for the research of other promising glass ceramic Li electrolytes. This gives the way to the energy density improvements of reported preliminary Li ion all solid state batteries based on phosphate materials [5]. Their development will be much more efficient if materials are selected, besides conventional electrochemical criteria, with respect to their chemical compatibility upon the sintering process. The search for materials with low sintering temperature will then enlarge the range of combinable materials. The electrode/electrolyte interface upon cycling can be ensured by considering electrode materials working with small volume change upon the electrochemical reaction.

The all solid state technology developed by SPS opens new field of investigations starting by the consideration of materials, which were disregarded for conventional liquid/polymer Li ion batteries. This should also begin by a new interest for solid electrolytes, which could fit all the requirements discussed above.

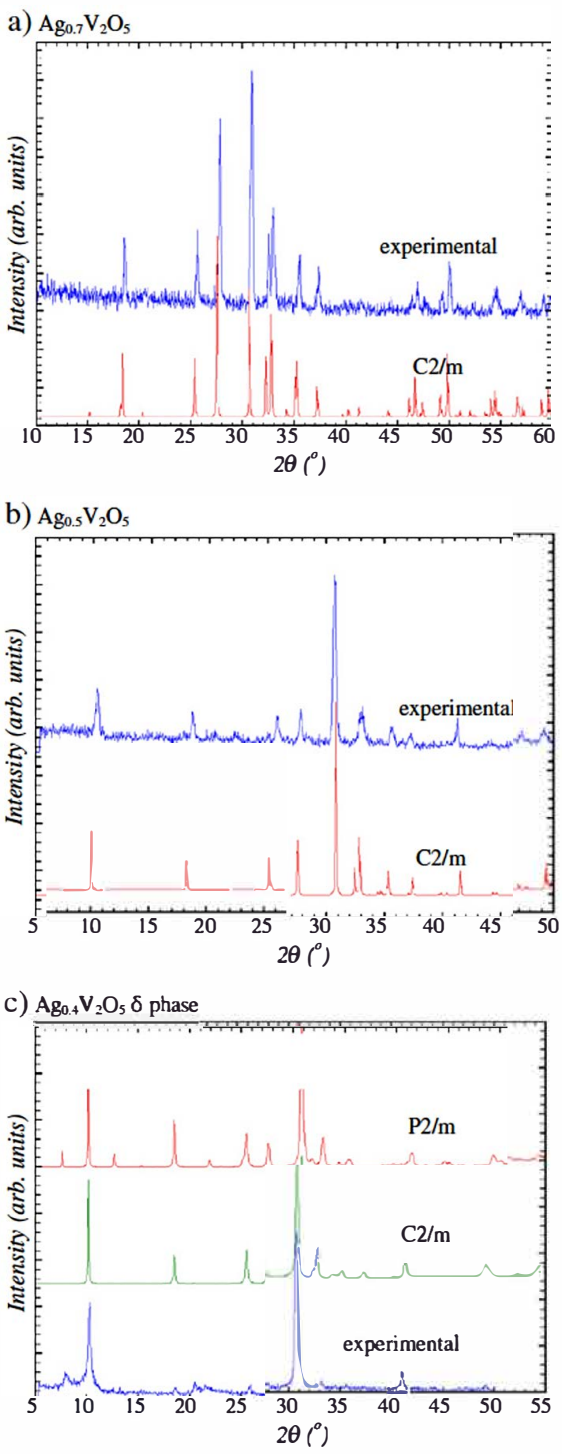

Fig. 9. X-ray diffraction pattern of chemical extracted phase from δ-$Ag_{0.7}V_2O_5$ and calculated pattern for the corresponding δ phase (a) $Ag_{0.7}V_2O_5$, (b) $Ag_{0.5}V_2O_5$ and (c) $Ag_{0.4}V_2O_5$ fitted with δ phase calculated parameters.

References

[1] B.B. Owens, P. Reale, B. Scrosati, Electrochem. Commun. 9 (2007) 694–696.
[2] O. Yamamoto, in: P.G. Bruce (Ed.), 1st Ed. Cambridge University Press, Cambridge, 1995, p. 292, 1995.
[3] K. Nagata, T. Nanno, J. Power, Sources 174 (2007) 832–837.
[4] J. Galy, M. Dollé, T. Hungria, P. Rozier, J.-P. Monchoux, Solid State Sci. 10 (2008) 976–981.
[5] A. Aboulaich, R. Bouchet, G. Delaizir, V. Seznec, L. Tortet, P. Rozier, M. Morcrette, J.-M. Tarascon, V. Viallet, M. Dollé, Adv. Energy Mater. 1 (2011) 179–183.
[6] T. Takahashi, S. Ikeda, O. Yamamoto, J. Electrochem. Soc. 120 (1973) 647–651.

[7] T. Takahashi, O. Yamamoto, S. Yamada, S. Hayashi, J. Electrochem. Soc. 126 (1979) 1655–1658.
[8] K. Takada, T. Kanbara, Y. Yamamura, S. Kondo, Solid State Ionics 40/41 (1990) 988–992.
[9] K. Takada, T. Kanbara, Y. Yamamura, S. Kondo, Eur. J. Solid. State. Inorg. Chem. 28 (1991) 533–545.
[10] J. Galy, J. Solid State Chem. 100 (1992) 229–245.
[11] P. Mondalek, L. Silva, L. Durand, M. Bellet, AIP Conference Proceedings, 1252, 2010, pp. 697–704.
[12] L.Y.Y. Chan, S. Geller, J. Sol. St. Chem. 21 (1977) 331–347.
[13] G. Delaizir, M. Dollé, P. Rozier, X.H. Zhang, J. of The American Ceram. Soc. 93 (2010) 2495–2498.
[14] F. Mizuno, A. Hayashi, K. Tadanaga, M. Tatsumisago, Solid State Ionics 177 (2006) 2721–2725.
[15] H. Kitaura, A. Hayashi, T. Ohtomo, S. Hama, M. Tatsumisago, J. Mater. Chem. 21 (2011) 118–124.